The CR Proton Spectrum measured with GRAPES-3

Fahim Varsi,
KIT-ETP

IAP-HEU Groups Seminar SS 2024

June 6, 2024

Karlsruher Institut für Technologie

KIT North campus

Table of contents

Introduction to cosmic rays (CRs)

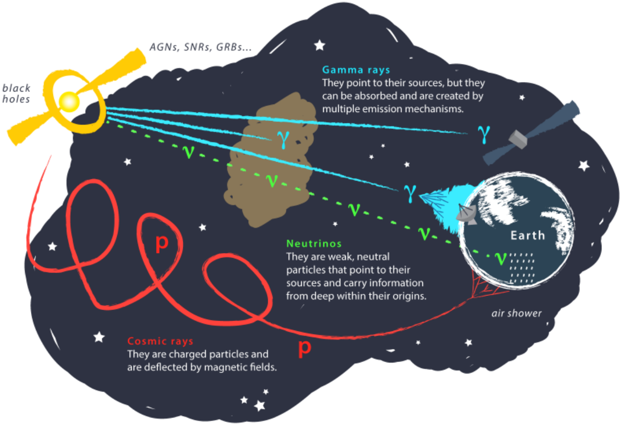

https://icecube.wisc.edu/news/view/455 (Juan Antonio Aguilar and Jamie Yang. IceCube/WIPAC)

- Cosmic Rays (CRs):
  - High-energy charged particles.
  - Energy: 10^{9} eV to 10^{20} eV.
  - ~90% protons, ~9% He nuclei and rest heavy nuclei & $e^{\pm}$.
- CRs diffuse by the interstellar magnetic field, not point back to sources.
- We lack the complete understanding of their sources and acceleration and propagation processes.
- Observables:
  - Energy spectrum.
  - Mass composition.
  - Anisotropy.
  - Multi-Messenger Astronomy.

CRs energy spectrum

- It follows a power law,

$$\Phi(E) = \frac{dN}{dE\, dA\, d\Omega\, dt} = K\, E^{-\gamma} \quad m^{-2} s^{-1} sr^{-1} GeV^{-1}$$

- Well-known features,
  - Knee at $\sim 10^{15}$ eV.
  - Ankle at $\sim 10^{18}$ eV.
  - GZK cut-off at $\sim 10^{20}$ eV.

J. Phys. G: Nucl. Part. Phys. **31** (2005) R95–R131 doi:10.1088/0954-3899/31/5/R02

TOPICAL REVIEW

Can diffusive shock acceleration in supernova remnants account for high-energy galactic cosmic rays?

A M Hillas

School of Physics and Astronomy, University of Leeds, Leeds LS2 9JT, UK

The first lesson from figure 1 is that a single component of cosmic rays appears to extend from below 10^{10} eV to at least 10^{16} eV in proton energy. To a good approximation a uniform spectrum in rigidity, $R^{-2.69}$, consistent with the expectations of a simple ('test particle') shock acceleration model, is quite acceptable: it fits also the total air shower flux around 10^{15} eV, and

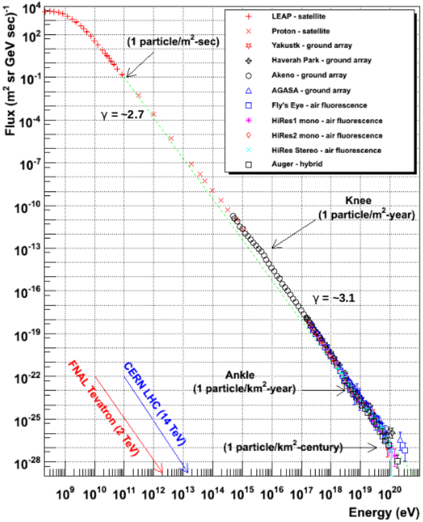

https://web.physics.utah.edu/whanlon/spectrum.html.

Motivation

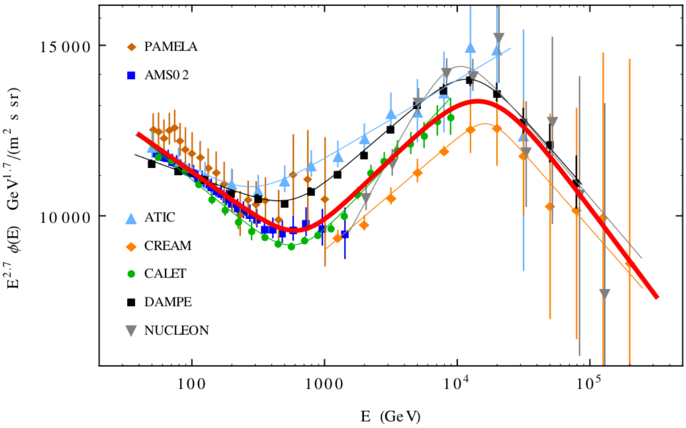

- Hardening and softening of CRs proton spectrum contradict the long-held belief of single power law before the Knee.

P. Lipari and S. Vernetto, Astropart. Phys. 120 (2020) 102441.

Motivation

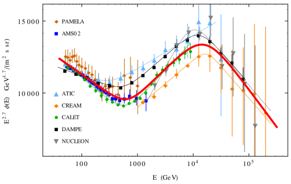

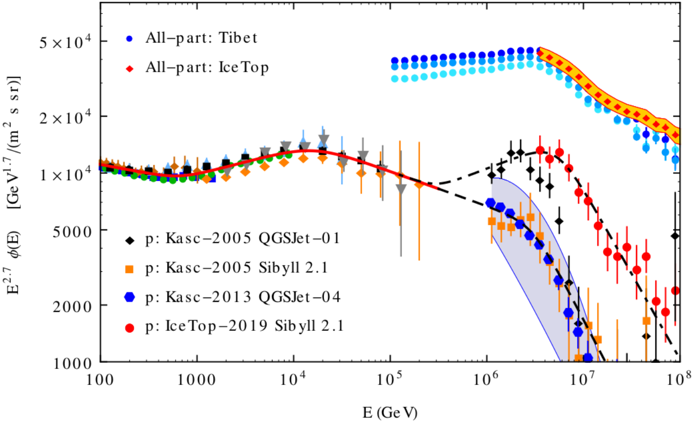

- Hardening and softening of CRs proton spectrum contradict the long-held belief of single power law before the Knee.
- Lack proton spectrum results from 100 TeV to PeV energy range.
- Non-unique extrapolation to higher energy.

P. Lipari and S. Vernetto, Astropart. Phys. 120 (2020) 102441.

The GRAPES-3 experiment

Location:

- Ooty, South India.
- 11.4° N, 76.7° E.
- 2200 m a.s.l.

- 400 plastic scintillation detectors cover an area of 25,000 m^2.
- Large tracking muon telescope of area 560 m^2.
- $\sim 3 \times 10^6$ extensive air showers (EASs)/day in TeV - PeV.

Scintillator Detectors (SDs) array

- Plastic SDs Array:
  - Total area: 25,000 m^2 with 400 plastic SDs (1 m^2).
  - 8 m inter-detector separation with Hexagonal geometry.
  - Samples relative arrival time (t) and density (ρ) of EAS charged particles.
  - Generates EAS trigger.
  - t → arrival direction (θ, ϕ).
  - ρ → shower parameters (N_e, s, x_c, y_c).

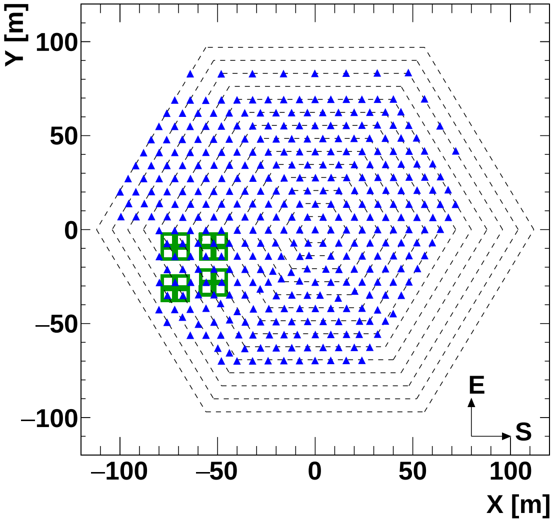

EAS direction and parameters reconstruction

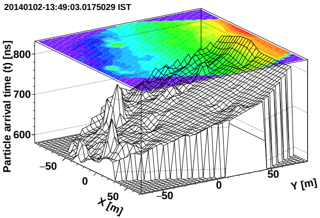

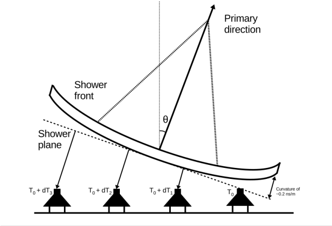

- Step 1: Plane fit to the shower front,

$$\chi^2 = \sum_{i=1}^{N} [lx_i + my_i + nz_i + c(t_i - t_0)]^2.$$

where N: number of triggered SDs,
x_i, y_i, z_i: coordinates of i^{th} SD,
t_0: time of shower front passes the origin,
c: speed of light,
l, m, $n(\theta, \phi)$ are the angle cosines.

- Step 2: Correct for shower curvature using shower size (N_e) and shower age (s).

V.B. Jhansi et al., JCAP07 (2020) 24.

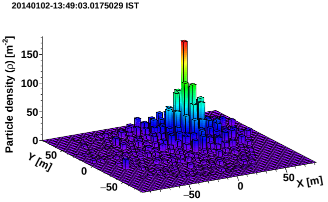

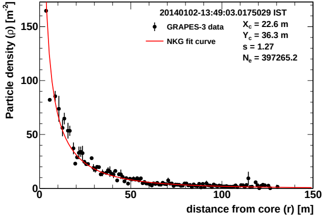

- NKG function,

$$\rho_i^{exp} = C \times \left(\frac{r_i}{r_0}\right)^{s-2.0} \left(1 + \frac{r_i}{r_0}\right)^{s-4.5},$$

$$C = \frac{N_e}{2\pi r_0^2} \frac{\Gamma(4.5 - s)}{\Gamma(s)\Gamma(4.5 - 2s)}.$$

where N_e: shower size → energy of CRs,
s: shower age parameter [0, 2],
r_0: Moliere radius (103 m for Ooty),
$r_i(x_c, y_c)$: distance of i^{th} SD from EAS core,
x_c, y_c: coordinates of EAS core.

GRAPES-3 muon telescope (G3MT)

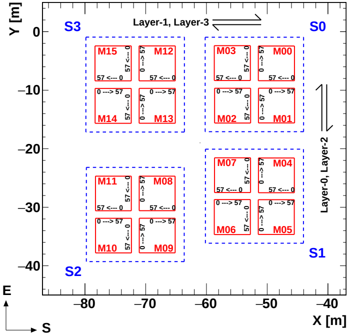

- Samples the muon component of EAS.
- 16 independent modules ($35\,m^2$); Total effective area: $560\,m^2$.
- Detector unit: proportional counters (PRCs).
- 4 adjacent modules (super-module) have separate DAQ but synchronized with EAS trigger.
- Concrete absorber ($550\,g\,cm^{-2}$).
- Energy threshold: $1\,GeV \times \sec\theta_\mu$, where θ_μ: muon incident angle.

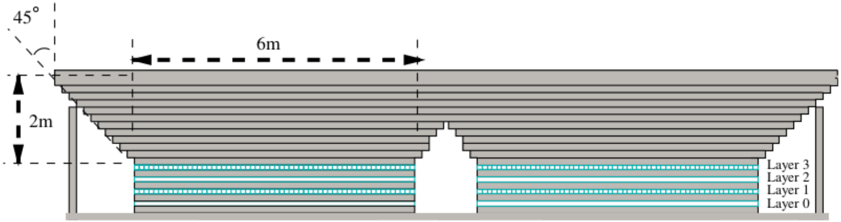

GRAPES-3 muon telescope (G3MT)

- PRC dimension: $6\,\text{m} \times 0.1\,\text{m} \times 0.1\,\text{m}$.
- Four orthogonal layers of PRCs.
- Layer-1 & 3 → X-Z plane;   Layer-0 & 2 → Y-Z plane.
- Discriminator threshold: 0.2 minimum ionizing particle (~4 keV).
- PRCs hit info → number of tracks/multiplicity (N_μ) → mass composition.

- Upper layer is scanned for a PRC hit starting from PRC number 0.
- Corresponding PRC hit in the bottom layer (according to projection of shower axis in the plane), along with ±1 PRC, is checked.
- Clustering of PRCs is considered once.

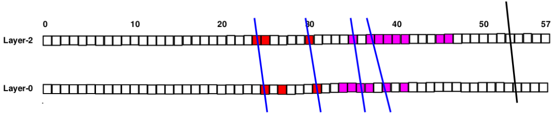

Monte Carlo (MC) simulations

- Detailed MC simulation study is done, which broadly involves,
  1. EAS development simulation in Earth's atmosphere using the CORSIKA package.
  2. Simulation of the EAS particles in the SDs to estimate their corresponding ρ and t.
  3. Detailed simulation of the EAS particles response in the G3MT using the GEANT4 package.

- EAS development simulation at GRAPES-3 site,
  - CORSIKA v7.6900 package.
  - QGSJET-II-04/FLUKA as high/low-energy hadronic interaction model.
  - H, He, N, Al and Fe.
  - E: 1 TeV to 10 PeV, with $E^{-2.5}$ spectral slope.
  - θ: 0° to 45°.
  - 6.1×10^7 EASs for each element.

- Simulation of the EAS particles in the SDs,
  - Analyzed with an in-house developed software framework.
  - Two datasets: dataset-1 with random core distributed within 150 m from array center for entire energy range, dataset-2 with 60 m from the center array for $E > 100$ TeV.
  - Each EAS used ten times with a random core location to improve statistics.
  - t ← CORSIKA output.
  - ρ ← GEANT-4 simulation of plastic SDs.
  - Generate EAS trigger and EAS parameters.

- Datasets with $E^{-2.7}$ spectral slope and proposed by GST and H4a composition models are derived.

Geant-4 simulation of G3MT: Geometric reconstruction

- GEANT4 simulation of G3MT involves,
  - Geometric modeling of the G3MT (PRCs and concrete absorber).
  - Passing sample of EAS particles from CORSIKA, followed by tracking and recording the energy deposited by the particle in the detector volume.

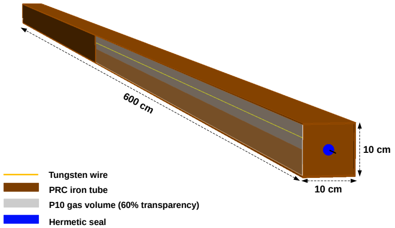

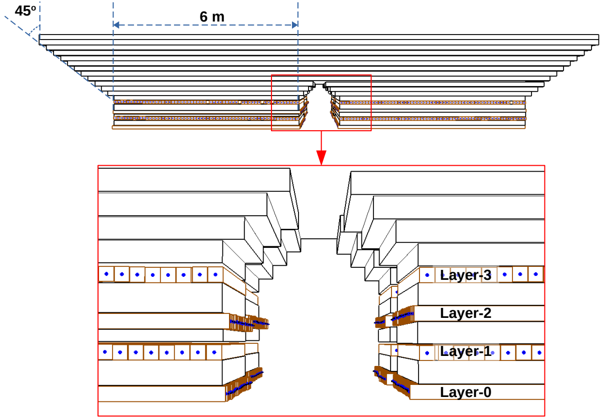

F. Varsi et al., JINST, 18 P03046 (2023).

Geant-4 simulation of G3MT: EAS particles response

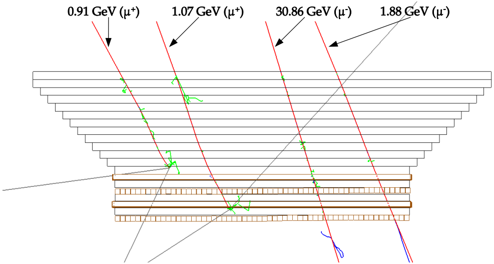

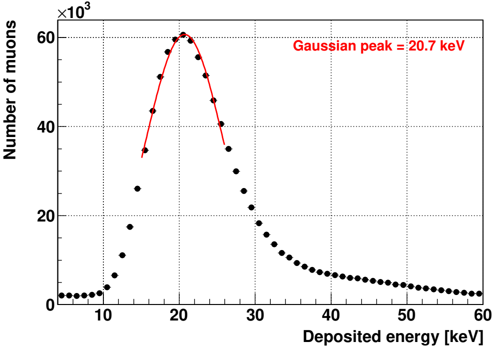

- Muons below 1 GeV$\times \sec\theta$ threshold absorb in the absorber.
- Muons above 1 GeV$\times \sec\theta$ threshold make a clear passage through the module.
- Energy deposited by single muons in PRC peaks at 20.7 keV; consistent with experimental value of ~20 keV.

Geant-4 simulation of G3MT: EAS particles response

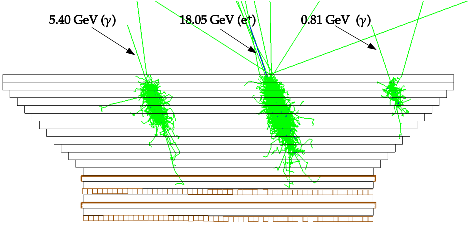

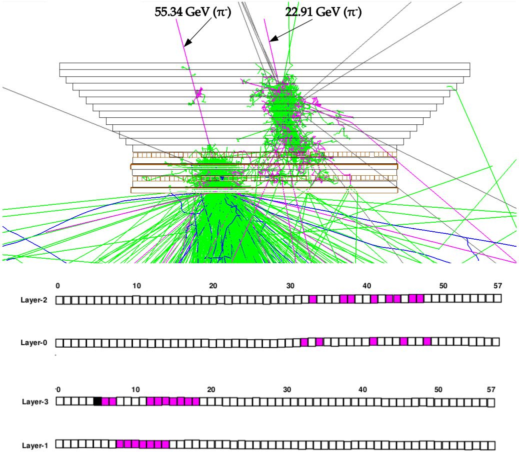

- Electromagnetic and low energy hadronic components get absorbed.
- High energy hadrons generate an EAS in the absorber, make complex PRC hits pattern.
- Multiple discrete PRC hits: more than one track.
- Clustering of PRC hits.

Hadron punch-through

- EAS hadrons generate shower inside concrete absorber, make complex PRC hits pattern.
- Hadron punch-through: fraction of number of tracks formed by hadrons.
- Hadrons are produced mostly closer to the shower axis; Their number falls rapidly with an increase in the distance from EAS core.
- ~10% at 20 m and reduces to ~2% at 60 m.

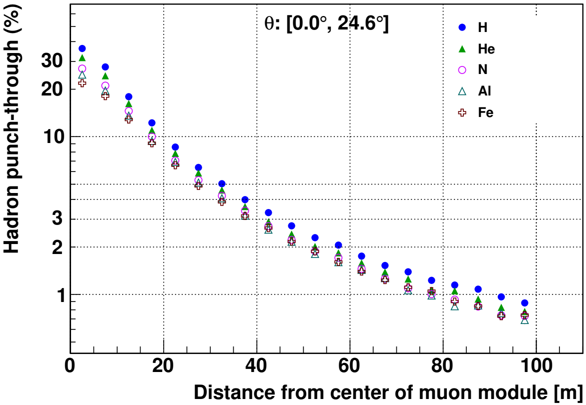

Selection quality cuts and data summary

- GRAPES-3 data: 1 January 2014 to 26 October 2015.

Quality cut	Number of surviving EASs	% of surviving EASs
1. Triggered	1.75×10^{9}	100.0
2. Abnormal days based on N_e spectrum	1.58×10^{9}	90.0
3. Successful event matching & muon tracking	1.17×10^{9}	66.8
4. Angle and NKG reconstruction	8.47×10^{8}	48.3
5. Shower age (s) between 0.02 and 1.98	8.41×10^{8}	48.0
6. Circular area within 50 m radius	3.96×10^{8}	22.6
7. Zenith angle < 17.8°	1.33×10^{8}	7.5
8. Hadron punch-through < 2%	6.27×10^{7}	3.6
9. $10^{4.0} \le$ Shower size (N_e) $< 10^{6.0}$	7.81×10^{6}	0.4

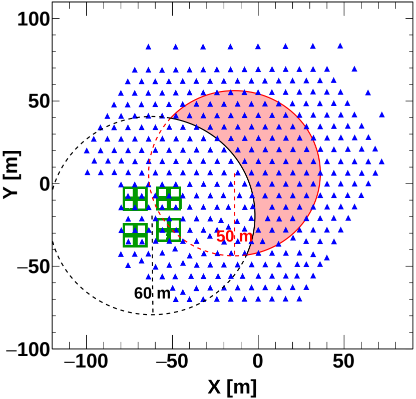

- Fiducial area: 4123 m^2

F. Varsi et al., Phys. Rev. Lett. 132, 051002 (2024).

Observed shower size distribution and live time

- For live time (T_{live}) calculation: distribution of inter-event time separation (Δt) fit with exponential function.

$$f(\Delta t) = Ae^{-R\Delta t},$$
$$T_{live} = N/R,$$

where R: time rate of the EAS passing the selection quality cuts, A: intercept and $N = 6.27 \times 10^9$ is the total number of EAS after the selection quality cuts.

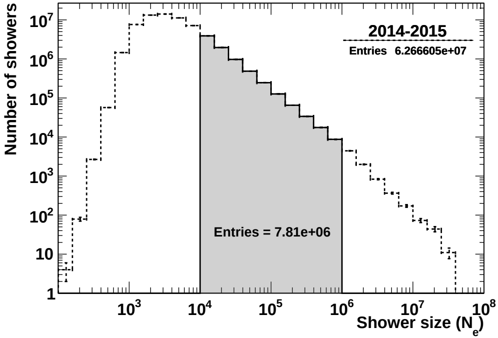

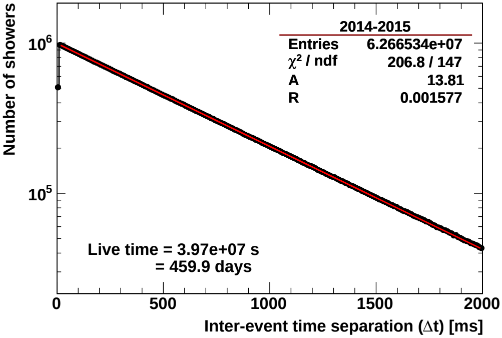

Trigger efficiency, total efficiency and acceptance of the GRAPES-3 array

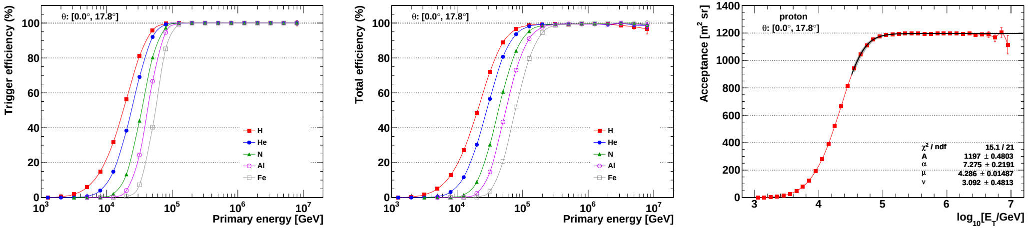

- ε_T reaches 90% at nearly 40 TeV, 45 TeV, 60 TeV, 70 TeV and 80 TeV for H, He, N, Al and Fe, respctively.
- ε_R nearly 100% above 200 TeV and total efficiency $(\varepsilon_{tot}) = \varepsilon_T \times \varepsilon_R$.
- Acceptance of GRAPES-3 array,

$$A_\Omega(E_i) = \frac{\pi A}{2}\varepsilon_{tot}(E_i)(\cos 2\theta_l - \cos 2\theta_u)$$

where $[\theta_l, \theta_u]$: upper and lower zenith angle range and A is fiducial area.

- $A_\Omega = \sim 1200\,\mathrm{m}^2$ sr for $\varepsilon_{tot} = 100\%$.
- Error in fit parameters are used to calculate the systematic uncertainty in the estimation of A_Ω.

Energy calibration and resolution

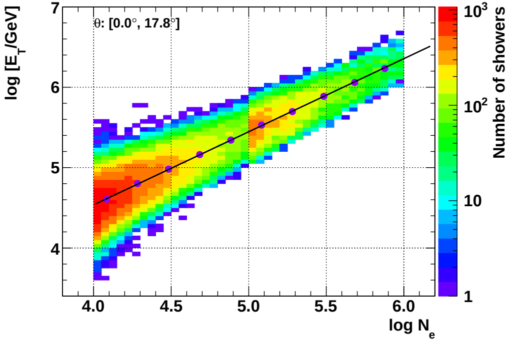

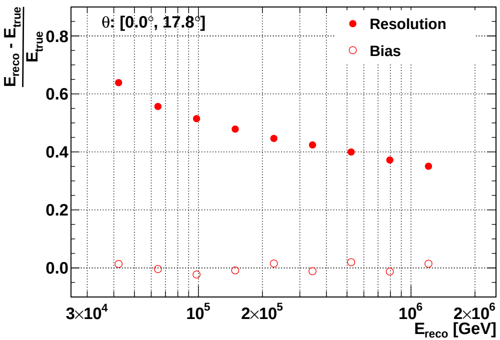

- Datasets with −2.7 spectral slope splited into 2 parts and first part was used for N_e and energy relation.
- Modeled with linear function on log-log scale.

$$\log E = p0 \times \log N_e + p1.$$

- Second parts was used to calculate distribution of $\frac{E_{reco} - E_{true}}{E_{true}}$.
- energy bias $=$ Median $\left(\frac{E_{reco} - E_{true}}{E_{true}}\right)$.
- energy resolution $= \sigma \left(\frac{E_{reco} - E_{true}}{E_{true}}\right)$.
- Bias within ±3% and resolution is 60% at 50 TeV and 35% at 1.3 PeV.

Muon multiplicity distribution (MMD)

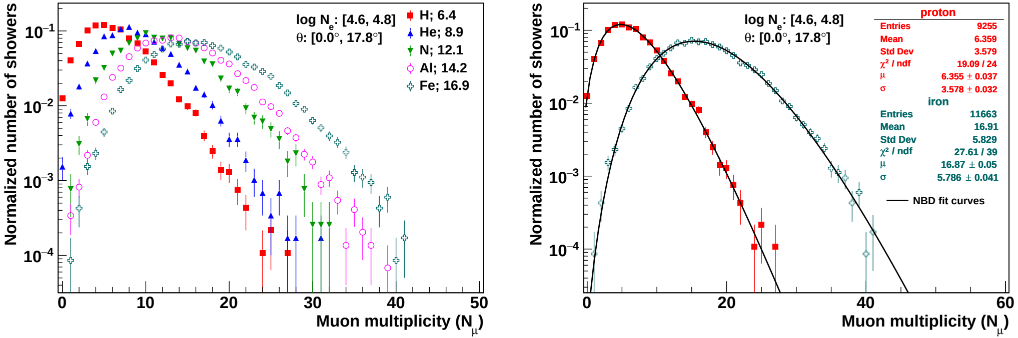

- The muon multiplicity distribution (MMD) is sensitive to the composition of the PCRs.
- Simulated MMDs fitted with negative binomial distribution (NBD).

$$NBD(N_\mu;\mu,\sigma) = \frac{\Gamma\left(N_\mu + \frac{\mu^2}{\sigma^2-\mu}\right)}{\Gamma(N_\mu+1)\Gamma\left(\frac{\mu^2}{\sigma^2-\mu}\right)}\left(\frac{\mu}{\sigma^2}\right)^{\frac{\mu^2}{\sigma^2-\mu}}\left(\frac{\sigma^2-\mu}{\sigma^2}\right)^{N_\mu},$$

- where μ is the mean value and σ is standard deviation of the MMD.

Paramterization of MMD

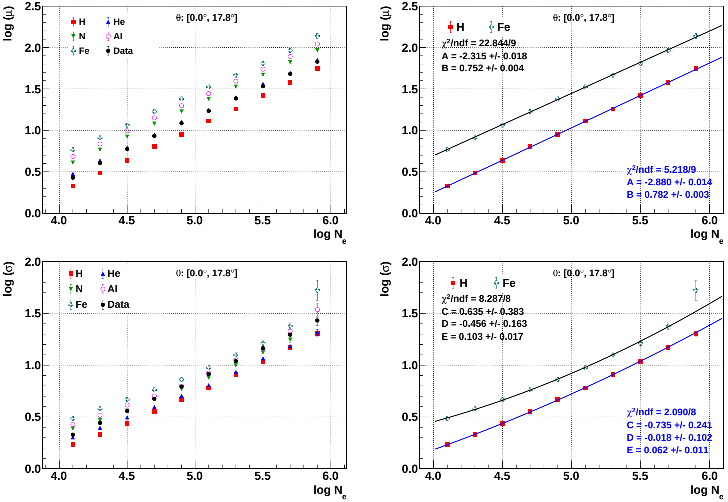

- μ and σ of observed data MMD is confined between corresponding fitted μ and σ for simulated proton and iron (extreme limits) primaries.
- μ: Linear function.

$$\log \mu = A + B \times \log N_e.$$

- σ: Quadratic function.

$$\log \sigma = C + D \times \log N_e + E \times (\log N_e)^2.$$

Mass composition: Gold's Unfolding algorithm

- Gold's unfolding procedure is employed twice.
  - Estimation of relative composition of each primary group from observed MMD for each shower size bin.
  - Estimation of the CR proton energy spectrum from the corresponding shower size distribution.

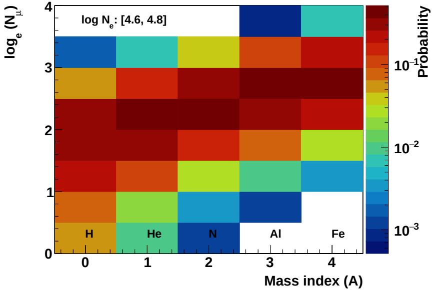

- For each N_e bin,
  - Response matrix $(\mathbf{R_1})$ generated from parameterization of MMDs.
  - Gold's iterative unfolding algorithm is used.

$$n(A_i^{k+1}) = n(A_i^k)\frac{(\mathbf{R_1}^T\mathbf{C}^T\mathbf{C}\vec{N}_\mu)_i}{\sum_j(\mathbf{R_1}^T\mathbf{C}^T\mathbf{C}\mathbf{R_1})_{ji}\, n(A_j^k)}.$$

where $C_{\alpha\beta} = \frac{\delta_{\alpha\beta}}{\sqrt{n(N_\mu)}}$.

  - Composition proposed by GST composition model used as prior.
  - Optimal stopping iteration: minimum of WMSE.

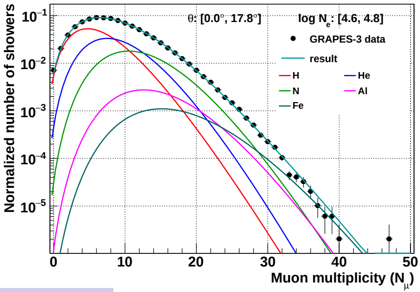

Relative composition of proton primary

- Relative composition of proton primary (a_1)
  1. $65 \pm 0.3^{+4.9}_{-6.8}$% at Ne $= 10^{4.1}$.
  2. $47 \pm 3.5^{+6.3}_{-10.5}$% at Ne $= 10^{5.9}$.

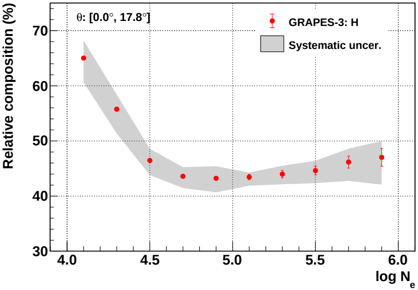

- Contribution from the following sources of systematic uncertainty is calculated.
  1. Unfolding algorithm (within 0% to 2%).
  2. Initial prior $\vec{A}$ (within ±1%).
  3. Bias from unfolding procedure (within −0.15% to +0.18%).
  4. Different spectral profiles to generate the response matrix (within +3.7%/−5.8% to +0%/−7.6%).
  5. Smoothing algorithm (within +0.7% to −4.1%).
  6. Limited statistics of MC simulations (from 3.2% to 6.0%).

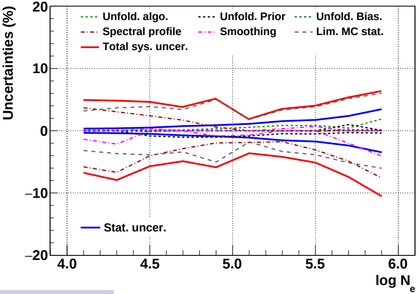

Proton size distribution and unfolding

- Observed N_e distribution (N_e^{obs}): convoluted distribution of different primaries.
- Proton N_e distribution (N_{e1}): Each bin of N_e^{obs} weighted with proton composition (a_1) in corresponding bin.

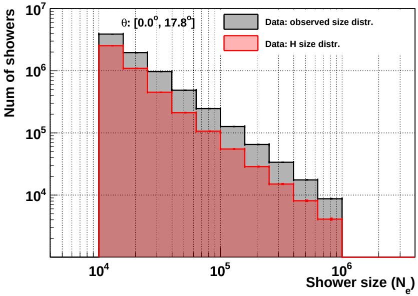

- Response matrix ($\mathbf{R_2}$) generated using simulation data with spectral slope of -2.7.
- Gold's algorithm is used iteratively as,

$$n(E_i^{k+1}) = n(E_i^k)\frac{(\mathbf{R_2}^T\mathbf{C}^T\mathbf{C}\vec{N}_e)_i}{\sum_j(\mathbf{R_2}^T\mathbf{C}^T\mathbf{C}\mathbf{R_2})_{ji}\, n(E_j^k)}.$$

- Initial prior selected with a spectral hardening near 200 TeV.
- Smoothing is applied on the $\vec{E}$ after each iteration.
- Optimal stopping iteration: minimum of WMSE.
- The final proton energy spectrum is not smoothened.

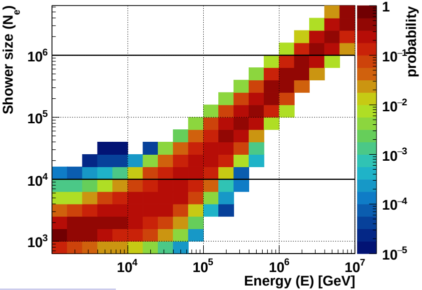

Proton energy spectrum

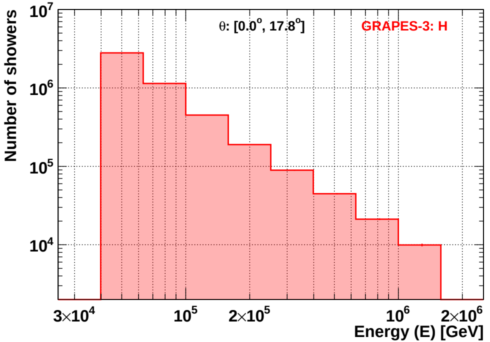

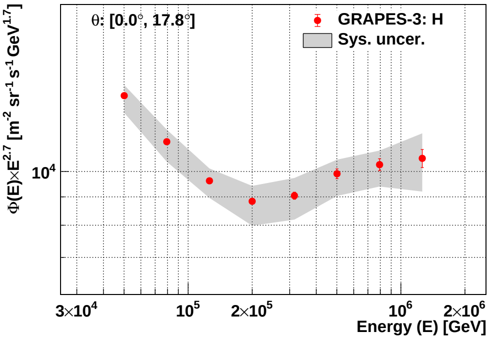

- Proton energy spectrum: 50 TeV to 1.3 PeV.
- The differential flux ($\Phi(E)_i$) for i^{th} energy bin is calculated from,

$$\Phi(E)_i = \frac{1}{T_{live}} \left(\frac{n(E_i)}{\Delta E_i \cdot A_{\Omega,i}} \right),$$

where $n(E_i)$: number of EAS in i^{th} energy bin, ΔE_i: bin-width of i^{th} energy bin, A_Ω: acceptance of GRAPES-3 array, T_{live}: live-time of GRAPES-3 data taking for this analysis.

- Scale with a factor of $E^{2.7}$ to show the spectral hardening near 165 TeV.

Proton energy spectrum

- Contribution from following sources of systematic uncertainty is calculated.
  1. Unfolding algorithm (within −0.02% to +0.11%).
  2. Initial prior $\vec{\vec{E}}$ (within −0.73% to +1.20%).
  3. Bias from unfolding procedure (within ±0.40%).
  4. Acceptance of GRAPES-3 EAS array (from 2.05% to 0.04%).
  5. Different spectral profiles to generate the response matrix (within −4.15% to +0.71%).
  6. Limited statistics of MC simulations (from 0.42% to 2.06%).
  7. Systematic uncertainty in relative proton composition (from +3.97%/−6.49% to +10.75%/−12.37%).

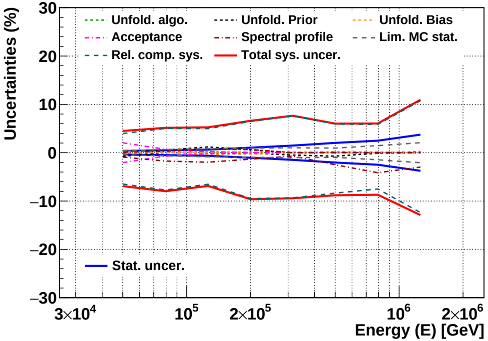

Modeling the spectral hardening

- Modeled with smoothly broken power law (SBPL), given as,

$$\Phi_S(E) = \Phi_0 \left(\frac{E}{50\ TeV}\right)^{\gamma_1} \left[1 + \left(\frac{E}{E_b}\right)^{\frac{1}{w}}\right]^{(\gamma_2-\gamma_1)\,w}$$

where Φ_0: flux normalization constant at 50 TeV,
E_b: energy corresponding to position of spectral break,
γ_1 and γ_2: spectral indices before and after E_b,
w: smoothness parameter for the spectral break.

- By considering only the statistical uncertainties during the modeling,

$$\Phi_0 = (1.370 \pm 0.005) \times 10^4\ m^{-2}\ sr^{-1}\ s^{-1}\ GeV^{-1},$$
$$E_b = 166.4 \pm 7.9\ TeV,$$
$$\gamma_1 = -3.12 \pm 0.02,$$
$$\gamma_2 = -2.56 \pm 0.02,$$
$$w = 0.22 \pm 0.06,$$

with $\chi^2/\text{ndf} = 3.36/3$.

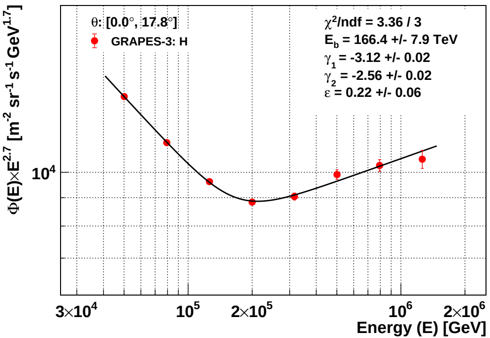

Significance the spectral hardening

- Null hypothesis: Modeled with single power law (PL), given as,

$$\Phi_P(E) = \Phi_0 \left(\frac{E}{50\ TeV} \right)^{\gamma}$$

- Alternate hypothesis: Modeled with SBPL.
- Test statistics (TS): χ^2_P - χ^2_S with 3 dof.
- For statistical uncertainties only,
  - $\chi^2_P = 897.90$ and $\chi^2_S = 3.36$.
  - TS $=$ 894.54 with 3 dof.
  - p-value $= 1.35 \times 10^{-193}$.
  - significance $(\sigma) = \phi^{-1}(1 - p) = 29.7\sigma$.
    where ϕ^{-1}: inverse of the cumulative distribution of the standard Gaussian.
- For statistical and systematic uncertainties,
  - $\chi^2_P = 18.67$ and $\chi^2_S = 0.16$.
  - TS $=$ 18.51 with 3 dof.
  - p $= 3.45 \times 10^{-4}$; $\sigma = 3.6\sigma$.

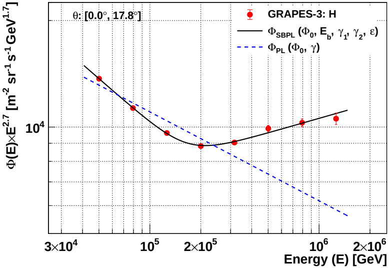

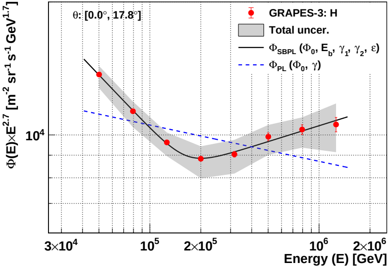

Proton energy spectrum

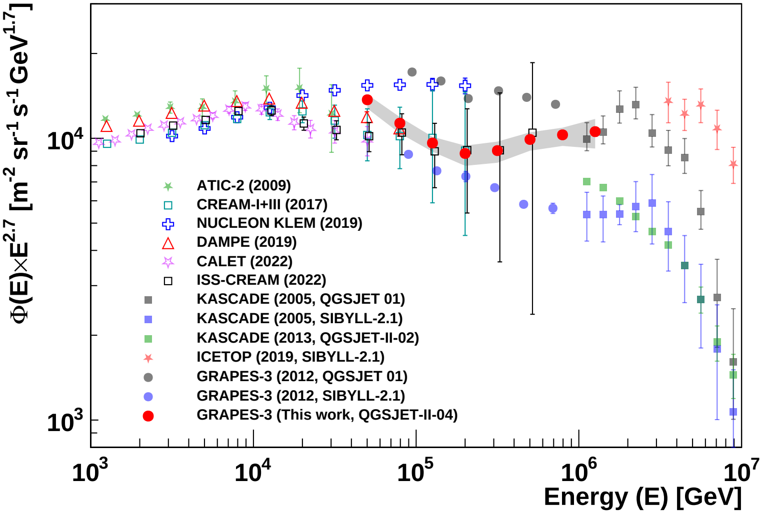

- At lower energy:
  - Good agreement with **ISS-CREAM**, **CREAM-I+III**, and **DAMPE**.
- At higher energy:
  - Good agreement with **KASCADE QGSJET 01**.

F. Varsi et al., Phys. Rev. Lett. 132, 051002 (2024).

Summary

- This work used MC simulation data based on QGSJET-II-04/FLUKA hadronic interaction models.
- For H, A_Ω saturates to ~1200 m^2 sr for $\theta < 17.8^\circ$ and fiducial area used in this analysis.
- Energy resolution for H is 60% at 50 TeV which improves to 35% at 1.3 PeV.
- The data recorded by GRAPES-3 from 1 January 2014 to 26 October 2015 was used, which contains 7.81×10^6 events after selection cuts.
- Proton energy spectrum is presented from 50 TeV to 1.3 PeV, providing the connection between direct and indirect measurements.
- Proton energy spectrum has a good overlap with direct experiments (ISS-CREAM. CREAM-I+III, DAMPE) at low energy and indirect experiment (KASCADE QGSJET 01) at high energy.
- Evidence of spectral hardening near 165 TeV is presented with a significance of 29.7σ by considering the statistical uncertainties and 3.6σ by considering the statistical and systematic uncertainties.

Thank you

Backup slides

Composition: Unfolding Vs Chi-Square minimization

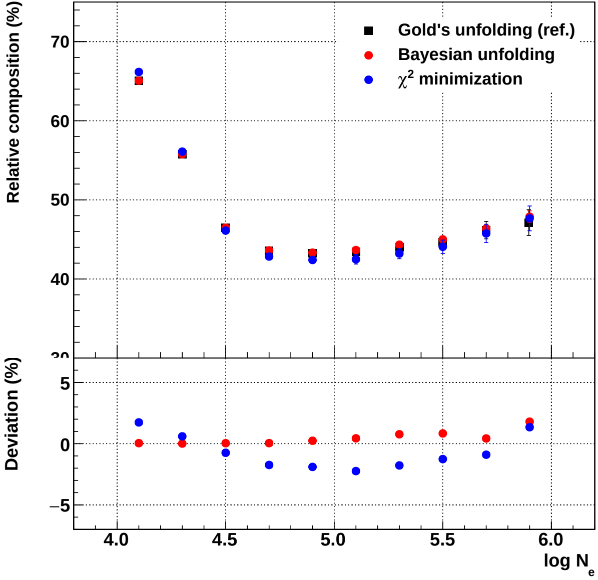

Gaussian randomization test: Simulation

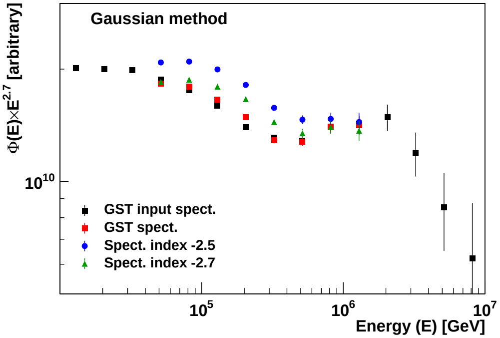

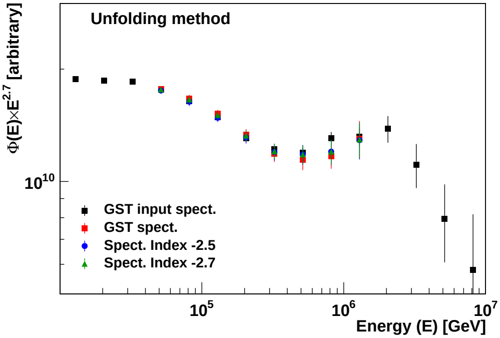

Gaussian randomization test: Data

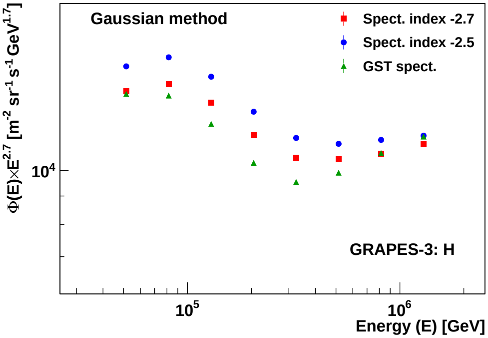

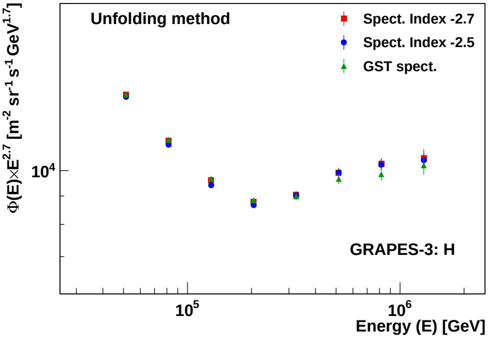

Muon saturation for different zenith angle and primaries

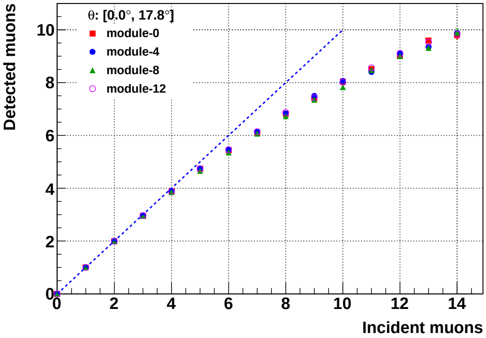

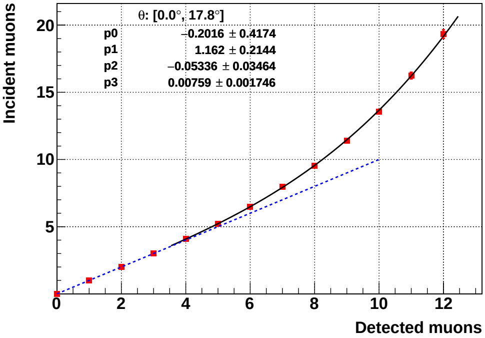

Muon saturation for different zenith angle and primaries

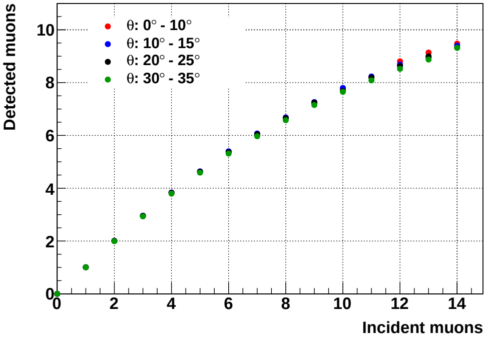

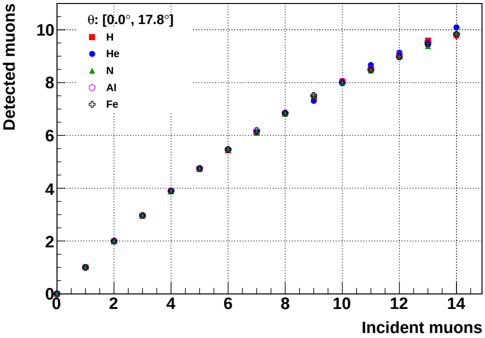

Hadron punch-through for different zenith angle and shower size bin

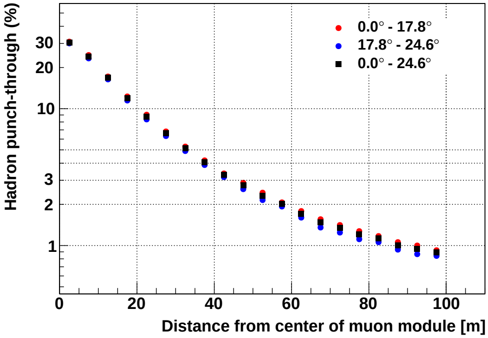

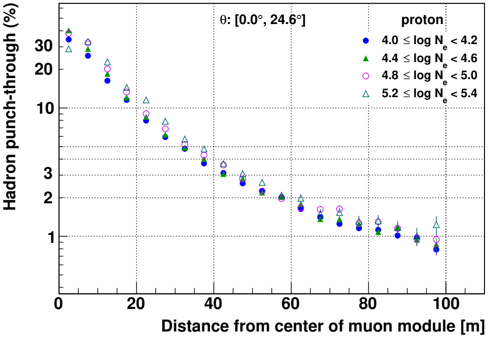

Core resolution

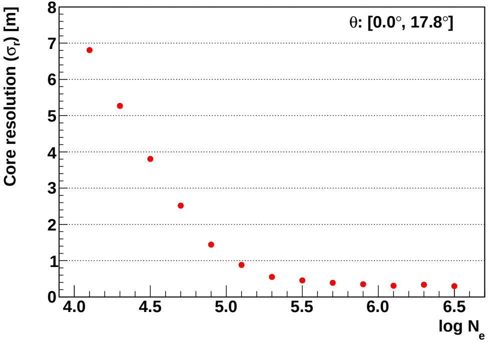

Reconstruction efficiency

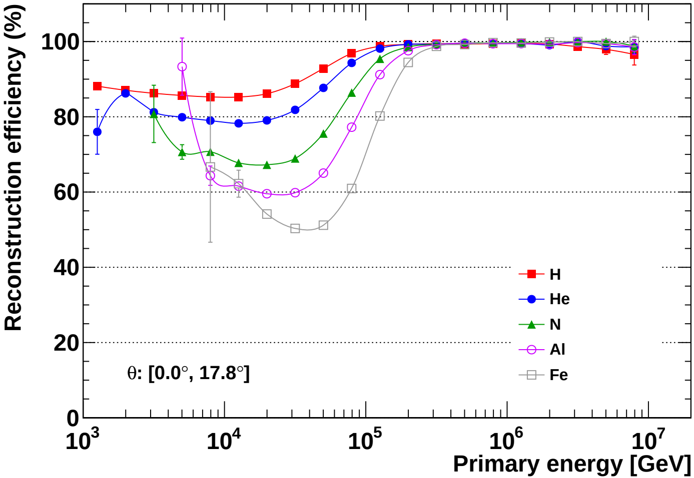

GST model

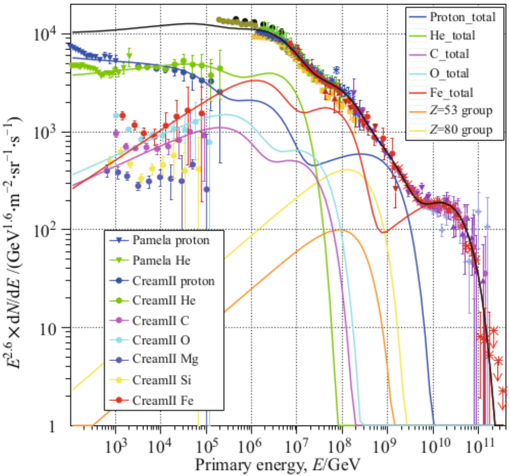

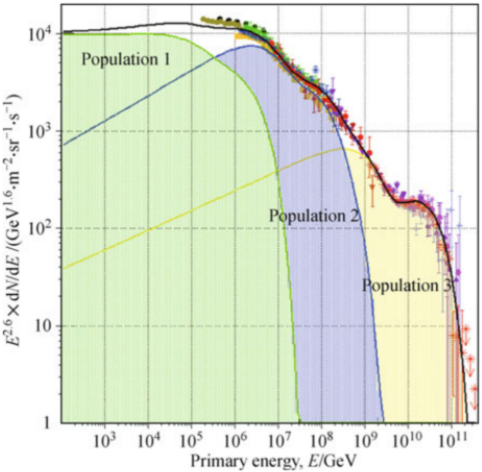

T. K. Gaisser, T. Stanev, and S. Tilav, Front. Phys., 2013, 8(6).

H4A model

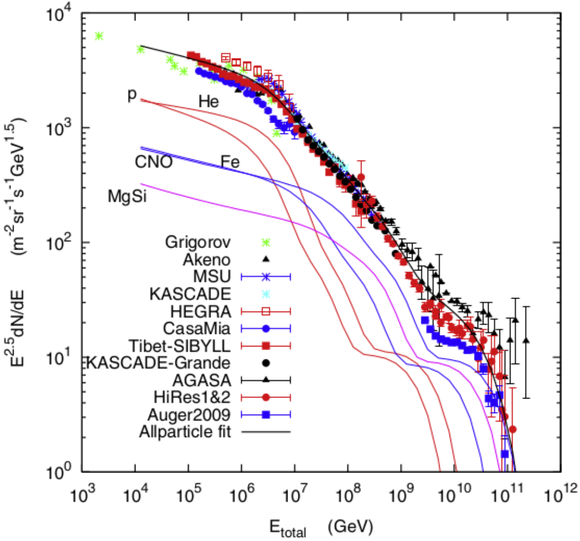

$$\phi_i(E) = \sum_{j=1}^{3} a_{i,j} E^{-\gamma_{i,j}} \times \exp\left[-\frac{E}{Z_i R_{c,j}}\right].$$

	p	He	CNO	Mg-Si	Fe
Pop. 1:	7860	3550	2200	1430	2120
$R_c = 4$ PV	1.66	1.58	1.63	1.67	1.63
Pop. 2:	20	20	13.4	13.4	13.4
$R_c = 30$ PV	1.4	1.4	1.4	1.4	1.4
Pop. 3:	1.7	1.7	1.14	1.14	1.14
$R_c = 2$ EV	1.4	1.4	1.4	1.4	1.4
Pop. 3(*):	200	0.0	0.0	0.0	0.0
$R_c = 60$ EV	1.6				

T.K. Gaisser, Astropart. Phys. 35 (2012) 801.

Check reliability of response matrix

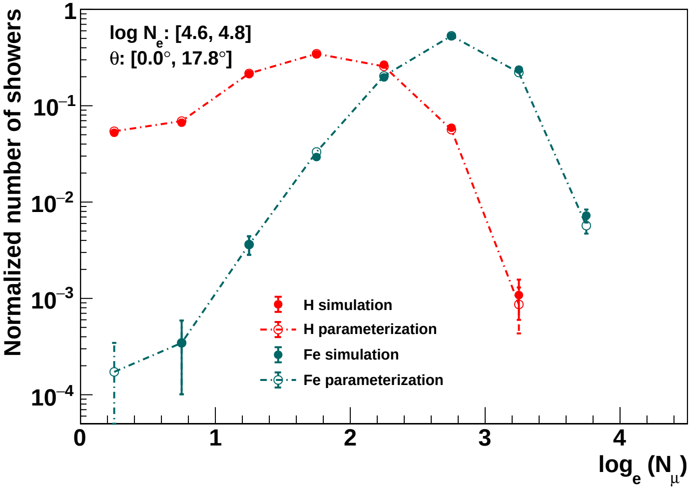

Propagation of systematic error in proton relative composition into energy spectrum

$$\frac{\partial E_{0,i}^{k+1}}{\partial a_{0,\alpha}} = E_{0,i}^{k+1}\left[\frac{1.0}{E_{0,i}^{k}}\frac{\partial E_{0,i}^{k}}{\partial a_{0,\alpha}} + \frac{1.0}{\overline{N}_{0f,i}^{k}}\left(\sum_{j}\frac{R_{\alpha j}R_{\alpha i}}{{}^{obs}N_{\beta}\, a_{0\beta}^{2}(1-f_{fake,\beta})}E_{0,j}^{k} - \sum_{j}R_{C,ji}\frac{\partial E_{0,j}^{k}}{\partial a_{0\alpha}}\right)\right],$$

$$\delta E_{0,i}^{k_0} = \sqrt{\sum_{\alpha}{}^{sys}\delta a_{0,\alpha}^{2}\left(\frac{\partial E_{0i}^{k_0}}{\partial a_{0,\alpha}}\right)^{2}}, \tag{7.21}$$